Gas Permeability Analysis of Photo-Cured Cyclohexyl-Substituted Polysiloxane Films

D. P. Dworak,[1] H. Lin,[2] B. D. Freeman,[2,3] M. D. Soucek[1]

[1]*Department of Polymer Engineering, The University of Akron, Akron, Ohio 44325*
[2]*Department of Chemical Engineering, University of Texas at Austin, Austin, Texas 78758*
[3]*Center for Energy and Environmental Resources, University of Texas at Austin, Austin, Texas 78758*

Received 27 June 2005; accepted 8 November 2005
DOI 10.1002/app.24480
Published online in Wiley InterScience (www.interscience.wiley.com).

ABSTRACT: A photo-cured cyclohexyl-substituted polysiloxane (PDCHS) film was prepared and compared with polydimethylsiloxane (PDMS) for the determination of permeability coefficients using various penetrants (H_2, N_2, O_2, CO_2, CH_4, C_3H_6, and C_3H_8). Penetrant sorption isotherms and local effective diffusion coefficients as a function of local penetrant concentration were also determined. The crosslink density of the films was measured via dynamic mechanical thermal analysis and was found to be 6.46×10^4 mol/m^3 for PDMS and 1.82×10^3 mol/m^3 for PDCHS. Photo-differential scanning calorimetry was used to calculate percent conversion under the conditions used for curing and was found to be (99.6 ± 0.3)% for PDMS and (98.4 ± 0.3)% for PDCHS. When cured, the PDCHS films had a lower crosslink density and lower permeance. It was postulated that the cycloaliphatic substitution along the polysiloxane backbone may not have full rotational ability affording closer intermolecular interactions, thus reducing the available free volume. © 2006 Wiley Periodicals, Inc. J Appl Polym Sci 102: 2343–2351, 2006

Key words: polysiloxanes; gas permeability; films; crosslink density; penetrants; P-DSC; DMTA

INTRODUCTION

Highly crosslinked polymeric films can be obtained through the photo-induced cationic polymerization of epoxides.[1,2] Polysiloxanes are well known for the extreme flexibility of the Si—O—Si bond and can be functionalized through the hydrosilation of Si—H and an alkene, specifically cycloaliphatic epoxy groups.[3,4] Hydrosilation can also be used to tailor the substituents on the polysiloxane backbone.[4–7] Polysiloxanes exhibit high chain packing density and the gas permeation performances of polymers are related to the structural properties and chemical composition of the membrane; thus polysiloxanes are of great interest for gas separation.[3] Consequently, poly(dimethylsiloxane) is a well-studied elastomer and has been commercially used to remove vapors such as propylene from mixtures with N_2. The structural properties (density, free volume, crosslink density, etc.) depend on the polymer, polymerization process, and conditions (temperature, photo-initiator concentration, viscosity, etc.).[8,9]

The permeability of a polymer to a gas A, P_A, is

$$P_A \equiv \frac{N_A\, l}{p_2 - p_1} \tag{1}$$

where N_A is the steady state flux of gas through the film, l is the film thickness, and p_2 and p_1 are upstream (i.e., high) and downstream (i.e., low) partial pressures of gas A, respectively.[10] According to Fick's law, if the downstream pressure is much less than the upstream pressure, the permeability is given by:

$$P_A = D_A \times S_A \tag{2}$$

where D_A is the average effective diffusivity through the film, and S_A is the apparent sorption coefficient:

$$S_A = \frac{C_2}{p_2} \tag{3}$$

where C_2 is the concentration of gas dissolved in the polymer when the gas pressure in contact with the polymer is p_2.[10] The ideal selectivity of a membrane for gas A over gas B is the ratio of their pure gas permeabilities:

$$\alpha_{A/B} = \frac{P_A}{P_B} = \left[\frac{D_A}{D_B}\right] \times \left[\frac{S_A}{S_B}\right] \tag{4}$$

where D_A/D_B is the diffusivity selectivity, the ratio of the diffusion coefficients of gases A and B.[10] The ratio of the solubilities of gases A and B, S_A/S_B, is the solubility selectivity. Diffusivity selectivity is strongly influenced by the size difference between the penetrant

Correspondence to: M. D. Soucek (msoucek@uakron.edu).

molecules and the size-sieving ability of the polymer matrix, whereas solubility selectivity is controlled by the relative condensability of the penetrants and the relative affinity between the penetrants and the polymer matrix.[10]

In this study, both a methyl and a cyclohexyl-substituted polysiloxane (PDCHS) (methyl-substituted MW $\sim$ 45,000 g/mol, cyclohexyl-substituted MW $\sim$ 35,000 g/mol) functionalized with cycloaliphatic epoxy and triethoxy silane groups were prepared.[4] The pendant triethoxy silane groups can undergo hydrolysis and condensation reactions to form crosslinks.[11,12] The homopolymerization of the cycloaliphatic epoxide groups was performed at ambient temperature via a cationic photo-initiator. Less condensable penetrants (i.e., H_2, N_2, O_2, and CH_4) and highly condensable penetrants (i.e., CO_2, C_3H_6, and C_3H_8) were used to approximate the permeability coefficients between the polydimethylsiloxane (PDMS) films and PDCHS films. The overall purpose of this work was to investigate the effects of bulky cyclohexyl groups on the permeability of penetrants though silicone membranes. Photo-differential scanning calorimetry (PDSC) was used to determine the degree of conversion of the two different films, since this would dramatically affect the permeability of the films. Dynamic mechanical thermal analysis (DMTA) was also performed to determine the crosslink density of the films.[13]

TABLE I
Physical Properties of Penetrant, Including Critical Volume (V_c),[14] Liquid Molar Volume at 35°C ($\overline{V}_2$),[15] Critical Temperature (T_c),[11] and Saturation Pressure at 35°C (p_{sat})[16]

	Size		Condensability	
Gas	V_c (cm^3/mol)	$\overline{V}_2$ (cm^3/mol)	T_c (K)	p_{sat} (atm)[a]
H_2	65.1		33	
N_2	89.8	48	126	(902)
O_2	73.4	47	155	(864)
CO_2	93.9	45	304	(82)
CH_4	99.2	46	191	(359)
C_3H_6	181.0	73	365	14
C_3H_8	203.0	80	370	12

[a] Values in parentheses are hypothetically extrapolated to 35°C, which is above the penetrant critical temperature.[13]

EXPERIMENTAL

Materials

Substituted polysiloxanes were synthesized and functionalized prior to this experiment.[4] Irgacure 250 was supplied by Ciba Specialty Chemicals and used as-received. Toluene (99.5%) was purchased from Aldrich Chemical Company and stored with molecular sieves (4 Å, beads, 8–12 mesh). Aluminum mill finish 2024-T3 (3×6 in.^{2}) panels were obtained from Q-panel.

Penetrants

Table I presents the physical properties of penetrants of interest (including penetrant size and condensability).

Film preparation and application

In a dry box the substituted polysiloxane ($\sim$ 3.0 g) was added to a glass vial, which was preheated at 100°C for 15 min prior to use. Dry toluene (20 wt %) was then added and thoroughly mixed. Irgacure 250 (3 wt %) was added and the entire solution was well mixed. The solutions containing PDCHSs required 6 wt % of Irgacure 250. With the aid of a draw down bar (8 mil), the solution was applied to acetone rinsed aluminum Q-panels that were treated with a mold release agent. A Fusion UV-curing chamber (F300SQ Series) with a belt speed of 25 ft/min was used to cure the polysiloxanes with a UV-source (mercury arc bulb, $\sim$ 150 mW/cm^2). Cured films were removed from the Q-panels 24 h after curing to allow for dark cure to complete. Samples for DMTA were prepared by curing a large drop of solution onto a Q-panel treated with a mold release agent. Cured samples were then lifted off and cut with a razor blade to the recommended size.

Photo-differential scanning calorimetry

On average, 2–3 mg of sample (polymer mixed with photoinitiator) was placed in an uncovered, hermetic, aluminum DSC pan. An empty pan was used as a reference. The chamber of the DSC was purged with nitrogen before the polymerization and was continued throughout the analysis. The samples were photocured with UV-light (150 mW/cm^2) for 15 s at 60°C to simulate the UV-curing chamber conditions. The heat flux as a function of reaction time was monitored under isothermal conditions, and the percent conversion was calculated.[14,15] The heat of reaction (ΔH_R) used for the epoxy group was 23.13 kJ/mol.

PDSC can be utilized to investigate the degree of conversion of the epoxy groups that participated in the homopolymerization.[16] The conversion can be calculated through the integral of the reaction rate profile:

$$\% \text{ Conversion} = (\text{Exotherm Area}(\text{J g}^{-1}) \times \rho)/(\Delta H_R \times [M]_0) \quad (5)$$

where ρ is the density of the solution, ΔH_p is the heat of reaction (kJ/mol), and $[M]_0$ is the initial concentration of epoxy groups.

Dynamic mechanical thermal analysis

Analysis of the viscoelastic response of the PDMS and PDCHS films was performed using a PerkinElmer PYRIS Diamond DMTA operating in compression mode. ASTM standard D 4065-95 was consulted for testing conditions and methodology. Samples were cut into 2.0 mm^2 samples and averaged 0.62 mm in thickness. The PDMS samples were analyzed over a temperature range of -150°C to 0°C while the PDCHS films were analyzed from -150°C to 100°C. Both films were run with a temperature ramp rate of 2°C/min. A minimum preload force of 200 mN and a center span deflection of 10 μm were applied by the instrument to the specimens. Frequency of testing was 1 Hz. The glass-transition temperature of the specimens was considered to be the peak point of the loss modulus (E″) signal. All analysis of raw data signals generated from the instrument was conducted using Perkin Elmer MUSE Standard Analysis V 3.6 U software.

DMTA was used to determine the crosslink density through the elastic modulus in the rubbery plateau region. The relationship between the rubbery plateau modulus and crosslink density, υ_e, is:

$$\upsilon_e = E/3RT \tag{6}$$

where E' is the tensile storage modulus (Pa), R is the ideal gas constant (J/K mol), and T is the temperature in Kelvin. The crosslink density is defined in terms of moles of network chains per cubic centimeter of sample. This route provides for reliable determination for crosslink density that is consistent with other mathematical approaches such as Graessley's.[17]

Film density

Polymer film density was determined by hydrostatic weighing using a Mettler Toledo balance (Model AG204, Switzerland) and a density determination kit.[18] In this method, a liquid with a known density (ρ_0) (the so-called auxiliary liquid) is needed, and the film density (ρ) is calculated as follows:

$$\rho = \frac{M_A}{M_A - M_L}\ \rho_0 \tag{7}$$

where M_A is the film weight in air and M_L is the film weight in the auxiliary liquid. An aqueous $Ca(NO_3)_2$ solution with a measured density of 1.412 g/cm^3 was used as the auxiliary liquid as a result of the PDCHS insolubility in water.[19] The film weight determination in the solution was performed as quickly as possible to reduce any swelling of the film due to water sorption.

Permeation measurements

The pure gas permeation properties for the PDCHS film were determined using a constant volume/variable pressure apparatus.[20] PDCHS samples were partially masked using impermeable aluminum tape on the upstream and downstream faces as described in previous studies.[21,22] The *o*-ring in the permeation cell was in direct contact with the aluminum tape so that the soft rubbery PDCHS film would not be damaged by the *o*-ring.

After a film was mounted in the system, both upstream and downstream volumes were exposed to vacuum overnight to degas the film. The leak rate in the system was always measured before starting the permeation experiments, and then the pressure increase in the downstream volume was recorded. Gas permeability (cm^3(STP) cm/(cm^2 s cmHg)) was calculated from the steady state rate of pressure increase in a fixed downstream volume:

$$P_A = \frac{V_d l}{p_2 ART}\left[\left(\frac{dp_1}{dt}\right)_{ss} - \left(\frac{dp_1}{dt}\right)_{leak}\right] \tag{8}$$

where V_d is the downstream volume (cm^3), l is the film thickness (cm), p_2 is the upstream absolute pressure (cmHg), A is the film area available for gas transport (cm^2), the gas constant, R is 0.278 cmHg cm^3/(cm^3(STP) K), T is absolute temperature (K), and $(dp_1/dt)_{ss}$ and $(dp_1/dt)_{leak}$ are the steady state rates of pressure rise (cmHg/s) in the downstream volume at a fixed upstream pressure and under vacuum, respectively. In this study, $(dp_1/dt)_{leak}$ was less than 1% of $(dp_1/dt)_{ss}$. The downstream pressure was always less than 2 cmHg, which was very low compared with the lowest upstream pressure considered ($\sim$ 4 atm).

Sorption measurements

Gas solubility was determined using a dual-volume, dual-transducer apparatus based on the barometric, pressure–decay method.[23] Uncertainty was estimated by a standard propagation of errors analysis, where uncertainties of all relevant measured parameters propagate and contribute to the uncertainty of the solubility.[24] Hydrogen solubility was too low to measure, and consequently, is not reported.

RESULTS AND DISCUSSION

Figure 1(a) and (b) depicts permeability coefficients of various penetrants in the PDCHS film at 35°C as a function of upstream pressure or pressure difference across the film. The detailed values are presented in Table II. In general, for less-condensable penetrants (i.e., H_2, N_2, O_2, and CH_4), permeability is essentially independent of pressure, while permeability coefficients of highly condensable penetrants (i.e., CO_2, C_3H_6, and C_3H_8) increase as penetrant pressure increases. This behavior is consistent with that of typical rubbery polymers, such as poly(dimethylsiloxane)

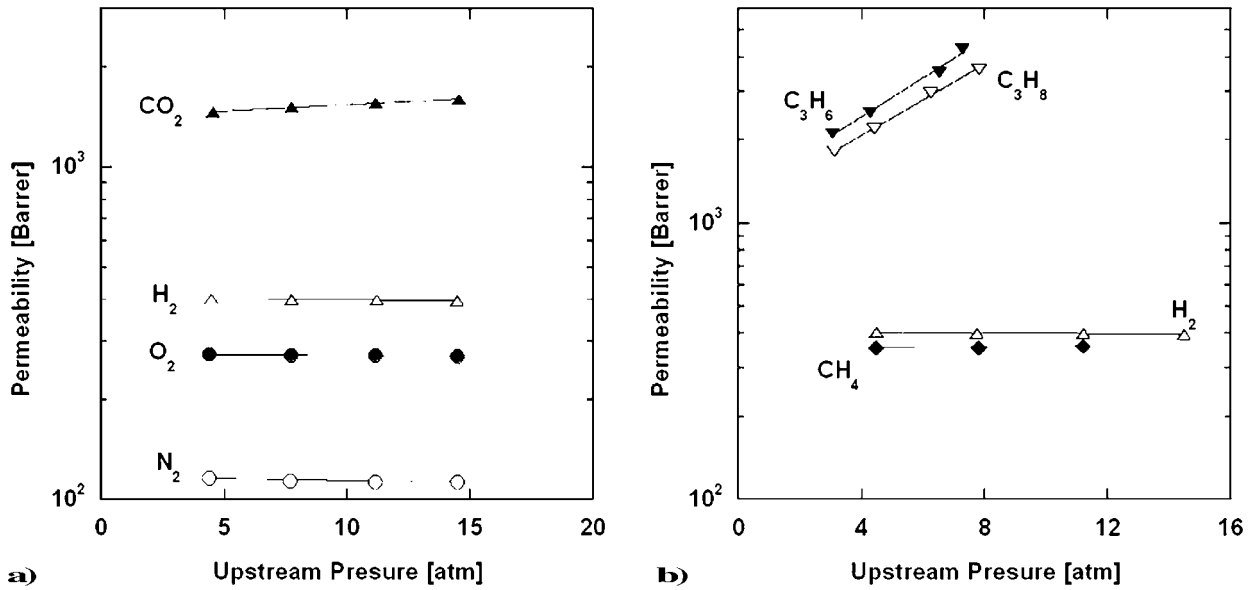

Figure 1 Permeability coefficients of penetrants (a) H_2, N_2, O_2, and CO_2 and (b) H_2, CH_4, C_3H_6, and C_3H_8 on poly(dicyclohexylpolysiloxane) at 35°C as a function of upstream pressure.

and poly(ethylene oxide).[13,23] Gas permeability is often related to gas pressure using the following empirical equation:

$$P_A = P_{A,0}\ \exp(m\Delta p) = P_{A,0}\ \exp(mp_2) \qquad (9)$$

where $P_{A,0}$ is the permeability coefficient at an upstream pressure, p_2, of 0 (i.e., infinite dilution permeability), m is an adjustable constant, and Δp is the difference between upstream pressure (p_2) and downstream pressure (p_1), $\Delta p = p_2 - p_1$.[25] Since p_1 is much less than p_2 in all our studies, Δp is approximated as p_2. The results are shown in Table III. In this way, a comparison in gas permeability can be made using $P_{A,0}$ without interference from the pressure effect.

Figure 2(a) is a comparison in permeability as a function of penetrant critical temperature. While permeability coefficients in PDMS are generally higher than those of the PDCHS, these two polymers exhibit a similar dependence of permeability on penetrant condensability (as represented by penetrant critical temperature, T_c). Permeability decreases in the following order:

$$CO_2 \approx C_3H_6 \approx C_3H_8 > H_2 \approx CH_4 > O_2 > N_2$$

Except H_2, which has a very small penetrant size, permeability increases with an increase in penetrant critical temperature. Figure 2(b) compares the ratio of gas permeability to N_2 permeability in both polymers. The selectivities are very similar in these two polymers which was expected due to the polysiloxane nature of both films.

Figure 3(a) and (b) depicts penetrant sorption isotherms in PDCHS at 35°C. The detailed values are shown in Table II. The polymer density, which is required to calculate gas concentration, was measured to be 1.037 g/cm^3. Gas sorption in noncros-

TABLE II
Gas Permeability and Concentration for Poly(dicyclohexylpolysiloxane) Film at 35°C as a Function of Pressure

Gas	Pressure (atm)	Permeability (Barrer)	Pressure (atm)	Concentration (cm^3(STP)/cm^3)
H_2	4.47	401		
	7.73	400		
	11.2	398		
	14.5	396		
N_2	4.40	116	3.73	0.265
	7.67	114	7.49	0.504
	11.1	113		
	14.5	113		
O_2	4.40	273	3.64	0.491
	7.73	272	7.05	0.913
	11.1	271	10.3	1.31
	14.5	270	13.9	1.78
CH_4	4.47	355	3.66	1.13
	7.80	355	7.01	2.16
	11.2	360	10.2	3.10
			13.4	4.034
CO_2	4.54	1460	3.07	3.29
	7.73	1520	6.10	6.55
	11.1	1560	9.20	9.92
	14.5	1600		
C_3H_6	3.04	2120	0.881	4.71
	4.27	2510	2.02	11.2
	6.51	3510	3.19	18.4
	7.26	4290	4.33	26.1
C_3H_8	3.11	1820	0.852	4.41
	4.40	2200	2.04	10.8
	6.24	2970	3.19	17.5
	7.80	3610	4.01	22.6

TABLE III
Summary of Permeability, Solubility, and Diffusivity Coefficients in Poly(dicyclohexylpolysiloxane) at 35°C

Penetrant	$P_{A,0}$	m (10^3) (1/atm)	$\frac{P_{A,0}}{P_{N_2,0}}$	S^∞ [cm^3(STP)/cm^3 atm]	$\frac{S_A^\infty}{S_{N_2}^\infty}$	χ	D_0 (10^6) (cm^2/s)	$\frac{D_{A,0}}{D_{N_2,0}}$
H_2	400 ± 27	−1 ± 13	3.3					
N_2	120 ± 8	−2 ± 13	1	0.07	1	1.0	12.9	1
O_2	270 ± 18	−1 ± 67	2.2	0.13	1.8	0.43	15.9	1.2
CH_4	350 ± 30	2 ± 10	2.9	0.30	4.3	0.49	8.7	0.67
CO_2	1400 ± 100	9 ± 7	12	1.04	15	0.77	10.4	0.81
C_3H_6	1270 ± 90	148 ± 14	10	4.89	70	0.45	2.0	0.16
C_3H_8	1150 ± 100	162 ± 15	9.6	5.00	71	0.54	1.8	0.14

slinked rubbery polymers is often described using the Flory–Huggins model:

$$\ln \frac{p}{p_0} = \ln \Phi + (1 - \Phi) + \chi(1 - \Phi)^2 \qquad (10)$$

where p_0 (atm) is the penetrant saturation vapor pressure at the temperature of the sorption experiment; it is estimated from the Antoine or Wagner equation and recorded in Table I.[11,26] The Flory–Huggins interaction parameter is χ, and Φ is the volume fraction of dissolved gas in the amorphous phase of the polymer, which is given by:

$$\Phi = C_2\overline{V}_2/(22{,}414 + C_2\overline{V}_2) \qquad (11)$$

where $\overline{V}_2$ is the partial molar volume of the penetrant (cm^3/mol), which is approximated as the mean value of the partial molar volume data reported by Kamiya et al.[27] The Flory–Huggins model might be used to describe gas sorption in lightly crosslinked polymers, since gas concentration in the polymers is typically low (i.e., less than 10 vol % in all studies here), and therefore, the elastic force of the network would not be significant. Flory–Huggins interaction parameter values were obtained by fitting experimental measurements of C_2 as a function of p_2 to eqs. (10) and (11). The curves in Figure 3(a) and (b) are drawn based on eqs. (10) and (11). It appears that a constant χ parameter is adequate to describe all the data.

Flory–Huggins interaction parameters for all penetrants are shown in Table III. Figure 4 also presents χ parameters in PDCHS, in comparison with those in PDMS. In general, the PDCHS exhibits slightly higher χ parameters than PDMS, indicating that the interactions between PDMS and penetrants are slightly less favorable than those between PDCHS and the corresponding penetrants. This could be attributed to the penetrants having more interaction/contact with the cyclohexyl substituents since they are considerably

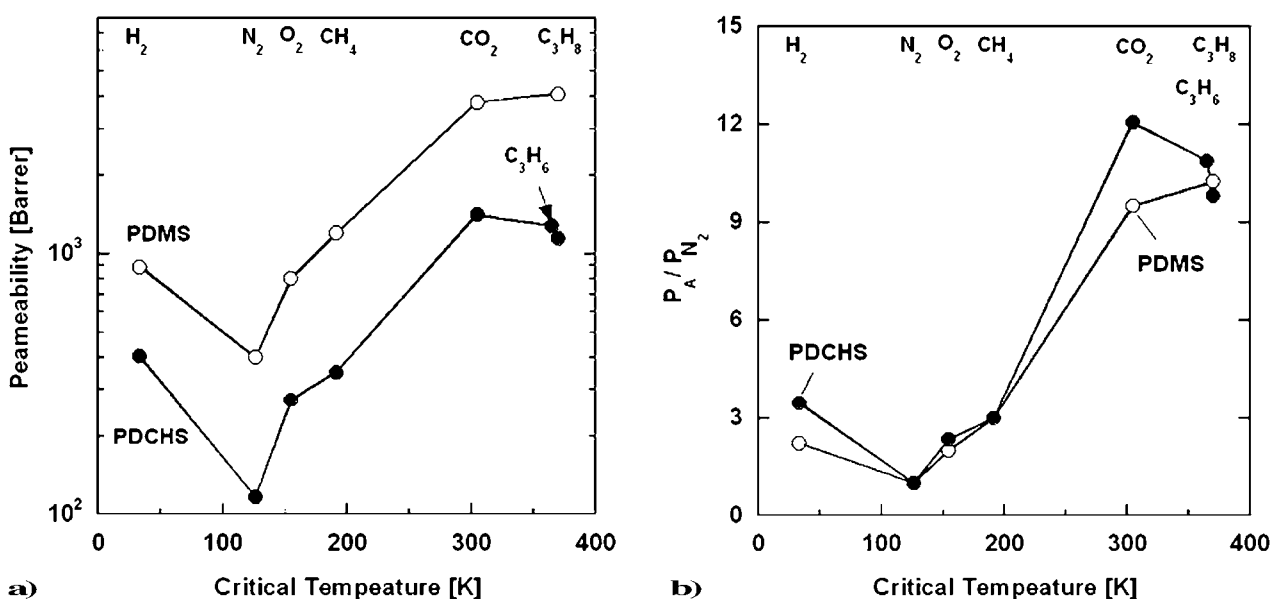

Figure 2 (a) Infinite dilution permeability of a poly(dicyclohexylpolysiloxane) film at 35°C as a function of penetrant critical temperature, compared with those in poly(dimethylsiloxane). (b) Ratio of infinite dilution permeability of various penetrants to that of N_2 on a poly(dicyclohexylpolysiloxane) film at 35°C as a function of penetrant critical temperature, compared with those of poly(dimethylsiloxane).

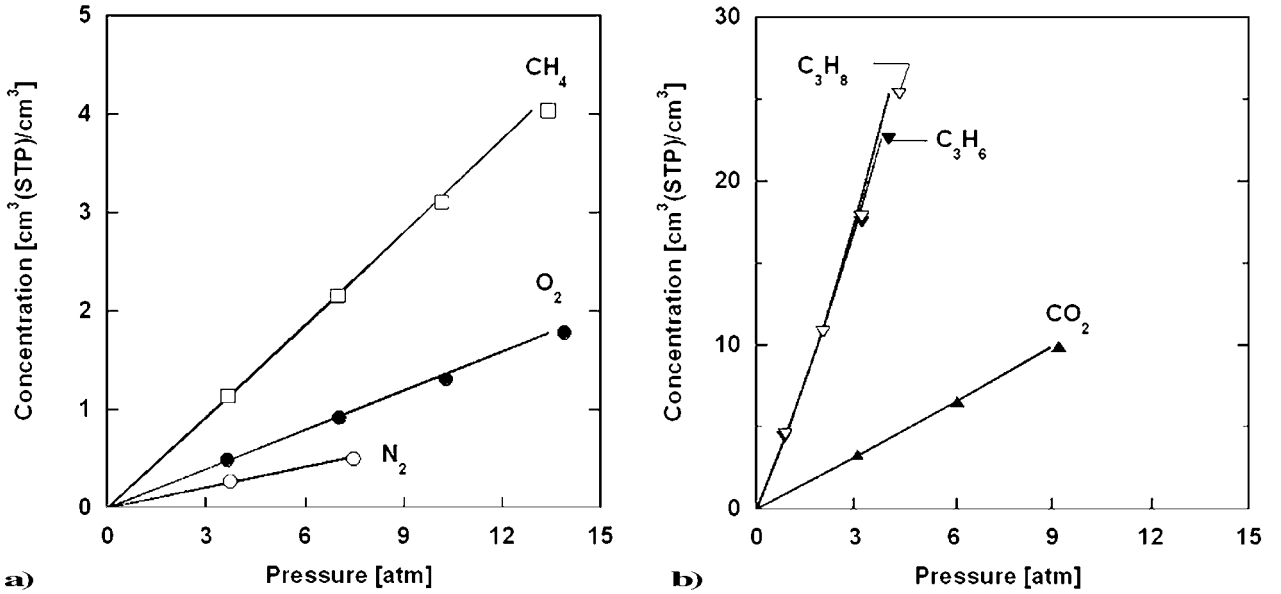

Figure 3 Sorption isotherms for (a) N_2, O_2, and CH_4 and (b) CO_2, C_3H_6, and C_3H_8 on a poly(dicyclohexylpolysiloxane) film at 35°C. The lines are modeled based on eqs. (10) and (11).

larger than methyl groups. At infinite dilution, eqs. (10) and (11) can be simplified to:

$$S^{\infty} = \frac{22{,}414}{p_0 \overline{V}} \exp(-1-\chi) \tag{12}$$

where S^{∞} is infinite dilution solubility of penetrants. The values of S^{∞} are calculated, shown in Table II, and presented in Figure 5(a) along with those in PDMS. Poly(dimethylsiloxane) films exhibit only slightly higher solubility. Therefore, the difference in gas permeability between PDCHS and PDMS should be primarily due to the difference in diffusivity. Figure 5(b) presents the ratio of gas solubility to N_2 solubility in both polymers. It seems that solubility selectivities are almost the same in these two polymers.

Local effective diffusion coefficients, D_{eff}, characterizing the penetrant diffusivity in the polymer at a penetrant concentration of C_2, can be evaluated using the following standard equation[23]:

$$D_{\text{eff}}(C_2) = \left[P_A + p\frac{dP_A}{dp}\right]_{p_2} \left(\frac{dp}{dC_2}\right)_{p_2} \tag{13}$$

Substituting eq. (9) in eq. (13) results in the following expression for the local diffusivity:

$$D_{\text{eff}}(C_2) = P_{A,0}(1+mp_2)\left(\frac{dp}{dC_2}\right)_{p_2} \tag{14}$$

The dependence of pressure on concentration could be derived from eqs. (10) and (11)[23]:

$$\left(\frac{dp}{dC_2}\right)_{p_2} = \frac{e^{\chi\Phi^2-2\chi\Phi-\Phi}}{S^{\infty}}(2\chi\Phi^2-2\chi\Phi-\Phi+1)\left(\frac{1}{1+C_2\overline{V}}\right)^2 \tag{15}$$

Figure 6(a) presents calculated effective diffusion coefficients in PDCHS as a function of local penetrant concentration. For all of the penetrants shown, D_{eff} increases with increasing local concentration, suggest-

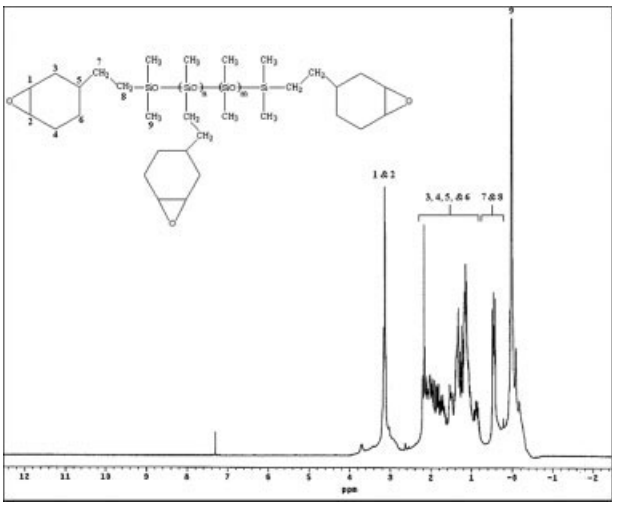

Figure 4 Flory–Huggins interaction parameters between penetrants and poly(dicyclohexylpolysiloxane) and poly (dimethylsiloxane) at 35°C as a function of penetrant critical temperature.

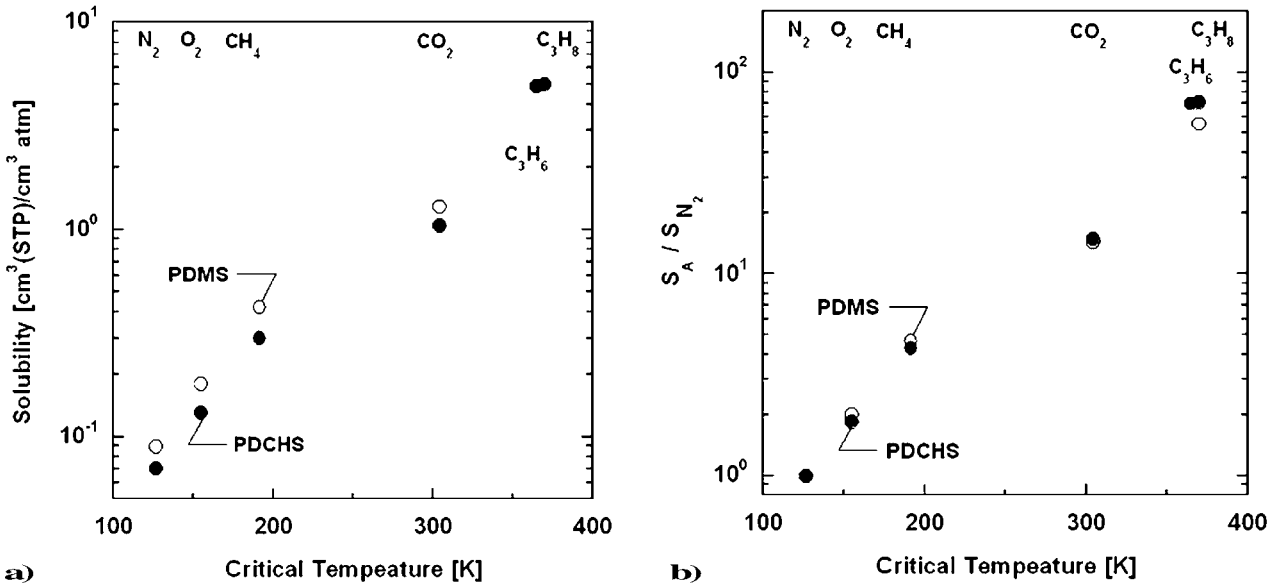

Figure 5 (a) Infinite dilution solubility in poly(dicyclohexylpolysiloxane) at 35°C as a function of penetrant critical temperature, compared with those in poly(dimethylsiloxane). (b) The ratio of gas solubility to N_2 solubility as a function of gas critical temperature.

ing that these penetrants plasticize the polymer matrix. This behavior is consistent with our previous argument that higher penetrant pressure can increase permeability by enhancing penetrant average diffusivity through the film. Figure 6(b) compares infinite dilution diffusivity (i.e., D_0) in PDCHS with those in PDMS. D_0 is calculated based on eq. (2) using the values of permeability and solubility at infinite dilution. Figure 6(b) reveals that PDMS exhibits higher diffusivity than PDCHS.

Since the degree of crosslinking within the films can have an effect on the permeability, PDSC was used to measure the degree of crosslinking and gauge the percent conversion of the epoxy groups along the polymer backbone. Table IV summarizes the results and shows that all three films have a percent conversion >98% and alleviate any possibility of comparison of membranes which have incomplete crosslinking. It was thought that the larger cycloaliphatic groups may have hindered the molecular

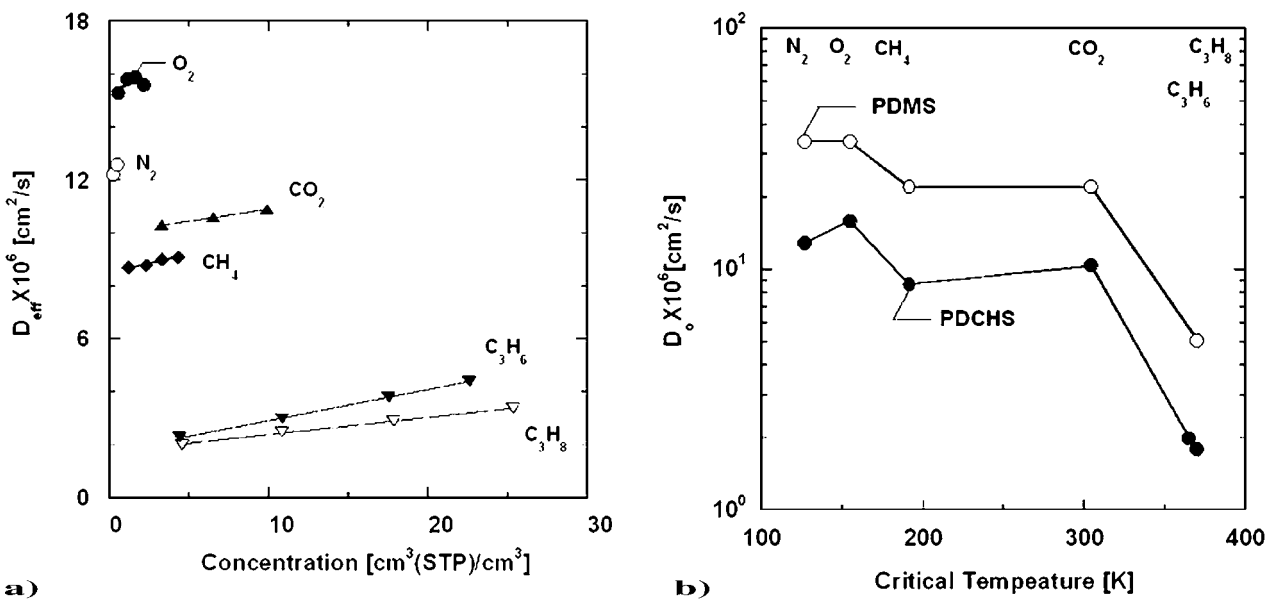

Figure 6 (a) Local effective diffusion coefficient in poly(dicyclohexylpolysiloxane) at 35°C as a function of penetrant concentration. (b) Infinite dilution diffusion coefficients of penetrants in poly(dicyclohexylpolysiloxane) and poly(dimethylsiloxane) at 35°C as a function of penetrant critical temperature.

TABLE IV
Summarization of Photo-Differential Scanning Calorimetry and Dynamic Mechanical Thermal Analysis Data

Substitution	E' (Pa)	T (K)	R (J/K mol)	v_e (mol/m^3)	% Conversion	T_g (°C)
Methyl	4.56E + 08	283.0	8.314	6.46E + 04	99.6 ± 0.3	−71.2
Cyclohexyl	1.65E + 07	363.0	8.314	1.82E + 03	98.4 ± 0.3	41.5

motion of the neighboring chains to allow for complete cure, however this was not the case.

The DMTA data reveals that the crosslink density (υ_e) for the methyl-substituted polysiloxane is higher than the cycloaliphatic-substituted polysiloxanes, which could be attributed to the smaller-sized methyl groups allowing for greater chain mobility and crosslinks during the polymerization process. The larger cycloaliphatic groups may restrain the number of crosslinks by obstructing the neighboring chains to come within close proximity. It was surmised that the methyl groups are small and chains can pack tightly within a network forming a higher crosslink density. However, the permeability was measured above the glass-transition temperature for the methyl system. Thus, it is not surprising that the methyl-substituted polysiloxane has a greater permeability [Figs. 2(a) and 6(b)], yet Table IV shows the crosslink density is higher.

Figure 7 illustrates the crosslinks in the PDMS and PDCHS films and depicts that although the cyclohexyl-substituted films shows a lower crosslink density the permeability is lower due to the presence of the large cycloaliphatic substituents acting as a ''barrier'' in the free volume of the network. It is proposed that the cycloaliphatic is impeded from fully rotating around 360° on account of steric hindrance. This allows closer packing between the polymer chains. The smaller methyl groups however freely rotate allowing for more free volume and penetrants to permeate through.

The gas permeability of the cyclohexyl-substituted films give insight on how bulky pendant groups affect the permeability of films and how this might be used in membrane development. The knowledge of the membranes composition and structure is crucial in developing successful membranes in that properties may be affected via poor conversion, obstructive pendant groups, or a low crosslink density. With more demanding membranes being developed for fuel cells and gas separation,[28,29] understanding of these variables will reveal new potential in the development of innovative membranes.

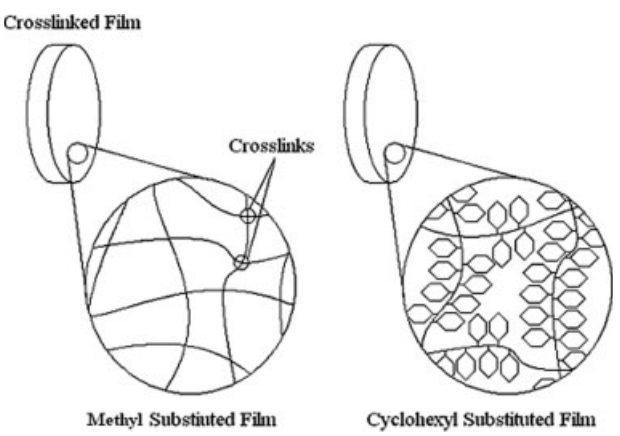

Figure 7 Depiction of higher crosslink density and higher permeance in poly(dimethylsiloxane) films.

CONCLUSIONS

Gas permeability studies, with various penetrants, were performed on crosslinked methyl- and cyclohexyl-substituted polysiloxane films. DMTA and PDSC were performed in tandem to confirm the results of the permeability studies. Both the PDMS and PDCHS films behave similarly in selectivity studies due to the polysiloxane nature of both films. The cycloaliphatic groups occupy more of the free volume between the crosslinks, which impedes the permeability of gases through the membrane even though the crosslink density for the PDCHS films are lower than the PDMS films.

The authors thank Steve Brenno of The University of Akron's Polymer Engineering department for his DMTA contribution.

References

1. Wicks, Z. W.; Jones, F. N.; Pappas, P. S. Organic Coatings Science and Technology; Wiley: New York, 1999.
2. Decker, C.; Nguyen Thi Viet, T.; Pham Thi, H. Polym Int 2001, 50, 986.
3. Smith, A. L. The Analytical Chemistry of Silicones; Wiley-Interscience: New York, 1991.
4. Dworak, D. P.; Soucek, M. D. Macromolecules 2004, 37, 9402.
5. Mowers, W. A.; Rajaraman, S. K.; Liu, S.; Crivello, J. V. In Technical Conference Proceedings, Baltimore, MD, April 9–12, 2000, Department of Chemistry, New York State Center for Polymer Synthesis, Rensselaer Polytechnic Institute, p 45.
6. Crivello, J. V.; Lee, J. J Polym Sci Part A: Polym Chem 1990, 28, 479.
7. Crivello, J. V.; Fan, M.; Bi, D. J Appl Polym Sci 1992, 44, 9.
8. Matsuyama, H.; Shiraishi, T.; Teramoto, M. J Appl Polym Sci 1994, 54, 166.
9. Yasuda, H. In Thin Film Processes; Vossen, J., Kern, W., Eds.; Academic Press: New York, 1978; Chapter 4.
10. Freeman, B. D.; Pinnau, I. In Polymer Membranes for Gas and Vapor Separation, Vol. 733; Freeman, B. D., Pinnau, I., Eds.; American Chemical Society: Washington, DC, 1999; p 1.

11. Soucek, M. D.; Ni, H. J Coat Technol 2002, 74, 125.
12. Teng, G.; Soucek, M. D. Macromol Mater Eng 2003, 288, 844.
13. Hill, L. W. Prog Org Coat 1997, 31, 235.
14. Harris, K. S.; Wang, C. M.; Bowman, C. N. Macromolecules 1994, 27, 650.
15. Guymon, C. A.; Bowman, C. N. Macromolecules 1997, 30, 1594.
16. Nelson, E. W.; Carter, T. P.; Scranton, A. B. J Polym Sci Part A: Polym Chem 1995, 33, 247.
17. Graessley, W. W. Adv Polym Sci 1974, 16, 108.
18. Zoller, P.; Walsh, D. Standard Pressure-Volume-Temperature Data for Polymers, 1st ed.; Technomic Publishing: Lancaster, PA, 1995.
19. Brandrup, J.; Immergut, E. H.; Grulke, E. A. Polymer Handbook, 4th ed.; Wiley: New York, 1999.
20. Bondar, V. I.; Freeman, B. D.; Pinnau, I. J Polym Sci Part B: Polym Phys 2000, 38, 2051.
21. Mogri, Z.; Paul, D. R. J Membr Sci 2000, 175, 253.
22. Lin, H.; Freeman, B. D. J Membr Sci 2004, 239, 105.
23. Bondar, V. I.; Freeman, B. D.; Pinnau, I. J Polym Sci Part B: Polym Phys 1999, 37, 2463.
24. Bevington, P. R.; Robinson, D. K. Data Reduction and Error Analysis for the Physical Sciences, 2nd ed.; McGraw-Hill: New York, 1992.
25. Stern, S. A.; Fang, S.-M.; Jobbins, R. M. J Macromol Sci Phys 1971, 5, 41.
26. Ghosal, K.; Freeman, B. D. Polym Adv Technol 1994, 5, 673.
27. Kamiya, Y.; Naito, Y.; Mizoguchi, K.; Terada, K.; Mortimer, G. A. J Polym Sci Part B: Polym Phys 1997, 35, 1049.
28. Yu, T.-L.; Lin, H.-L.; Shen, K.-S.; Huang, L.-N.; Chang, Y.-C.; Jung, G.-B.; Huang, J. C. J Polym Res 2004, 11, 217.
29. Xiang, T.-X.; Chen, J.; Anderson, B. D. J Membr Biol 2000, 177, 137.